Instabilities in a spherical liquid drop

Roger Prud'Homme

Instabilities in a spherical liquid drop[1]

Roger Prud'homme

Emeritus Research Director, UMR 7190 - Sorbonne-University / National Center for Scientific Research - Box 162 - 4 place Jussieu - 75252 Paris Cedex 05

Plan of the article 1

Abstract: We examine cases of stationary vortices that can appear inside spherical liquid drops in microgravity conditions. The first case is that of an incompressible external flow of uniform speed at infinity, leading the liquid in the drop by friction to form a Hill vortex. In the second case, the external fluid does not interact by friction with the liquid, but the drop is subjected to an axial temperature gradient causing a variation in surface tension. This time it is the induced movement which entrains the internal liquid. Note that the two situations can lead to the same Hill vortex. Combined effects are envisioned. We are also interested in the time factor in these phenomena.

Key words : liquid drops, instabilities, velocity field, thermal field, Hill vortex

[1] Paper proposed to Frontiers for "Transport Phenomena in Microgravity", October 13, 2021

List of symbols

Symbol	Meaning	Symbol	Meaning
D	Flow rate of a source	(x, y, z) (x_1, x_2, x_3)	Cartesian coordinates
$(\vec{\mathbf{e}}_r, \vec{\mathbf{e}}_\theta, \vec{\mathbf{e}}_\phi)$ $(\vec{\mathbf{i}}, \vec{\mathbf{j}}, \vec{\mathbf{k}})$	Unit basic vectors	$Y_l^m(\theta, \phi)$	Spherical harmonic
K	Intensity of a doublet	$\alpha, \alpha_e, \alpha_i$	Stream function coefficients
$\vec{\mathbf{n}}$	Unit normal	ε	Deformation rate
p, p_∞	Pressure, *p* at infinite	Γ	Intensity of an irrotational vortex
$P_{l,m}$	Legendre polynomial	$\mu, \nu = \nu/\rho$	Shear viscosity coefficients
r, θ, ϕ	Spherical coordinates	$\xi = \cos\theta$	Intermediate variable
R	Gas constant, radius of a sphere	ρ	Volumic mass
s	Curvilinear abscissa	σ	Surface tension
S	Surface	Ω	Rotation speed
T	Absolute temperature	$\vec{\boldsymbol{\omega}}$	Swirl vector
$\vec{\mathbf{t}}$	Unit tangent	ψ	Stream fonction
U, U_∞	Velocity at surface, velocity at infinity	i, e	Flow resp. internal external
$\vec{\mathbf{v}}, v = \lvert\vec{\mathbf{v}}\rvert$	Velocity vector, Velocity modulus	t, n	Resp. tangent, normal to the sphere of radius r
(u, v) or (v_r, v_θ)	Components of the velocity vector	r, θ	Resp. radial, tangential

1. Introduction.

The drops of the sprays undergo various actions depending on their origin and the resulting physical situation in which they are found, such as watering spray, medical spray, automotive engine injector, rocket engine injector, etc. Their modeling includes on the one hand the examination on the scale of each individual drop, and on the other hand the study of the spray itself on a larger scale, as a constituent of a multiphase flow which is most often liquid-gas. Individual drop is often considered to be spherical. This is the case with small drops where capillary efforts are decisive for the establishment of sphericity. This simplicity of geometric shape is called into question in the case of large drops and as soon as they are subjected to significant forces of aerodynamic origin for example.

For the sake of simplicity, we try during theoretical research to keep the spherical shape as long if possible.

*The **microgravity** can be considered as a factor favorable to the spherical shape of the drops of average size which can allow experimental observation.*

*Finally, the study is also interested in applications to **launchers**. This dual fundamental / applied aspect makes the study of sprays a reason of choice recommended by CNES within the framework of Material Sciences. [2]*

The exchanges between the individual drop and its gaseous environment are obviously different depending on whether there is evaporation-condensation or not. They concern the masses of the constituents, the momentum, and the energy. Each phase involved also undergoes motions and transfer phenomena.

For the flow of the spray itself, it is often necessary to model what happens inside the individual drops. The most classic is to characterize the latter by their radius, their mass, their temperature and their speed. The distribution in diameter and speed of the drops will always remain the essential element.

Nevertheless, it may be interesting to take care of the internal motions of medium-sized drops because these act on the exchanges at their surface. This is the problem that is proposed in this article, where we will therefore have to simultaneously study the external and internal flows of individual drops.

We have retained here the case of spherical liquid drops subjected either to a uniform external gas flow, or to a thermal gradient in an axial direction. We will see that Hill's vortex modeling is an interesting solution for interior flows.

One of the major problems is that of the connection between the flow inside the drop-limiting sphere and the flow of the outside fluid.

Indeed, if we assume a perfect fluid on the outside, we can logically be led to admit perfect sliding conditions for this fluid at the level of the surface of the drop. But then how to admit that there is entrainment of the internal liquid in the drop by the external fluid?

The problem of the forces exerted on the drop by the external fluid is also posed regarding their resultant which is found to be zero! This constitutes *the famous Dalembert paradox*. We are then invited to consider the viscosity of the external fluid, at least in the

[2] Indeed, linking work on microgravity research and space technologies is one of the objectives of the recommendations made during the CNES scientific prospective seminar in July 2004.

close vicinity of the sphere, which leads to Stokes' theory in the case of the rigid sphere. The results must also be modified to consider a liquid sphere. And in the presence of evaporation-condensation of the liquid it is even more complicated!

Finally, we know that for many linear problems one can superimpose elementary solutions. We will do this whenever possible, considering the nature of the fluids and the areas of validity that are the interior and exterior of the drop.

The origin of our study is related to the problem of combustion instabilities in rocket engines: It is established that the evaporation of droplets during combustion is the cause of amplification of HF vibrations generated by the engine (This model is mentioned in the appendix.). A feeded drop model was developed to represent the evaporating spray being. This model results from an improvement of that of Heidmann which did not consider the internal irreversibilities of the drop in evaporation. But if this model, with spherical symmetry, is well adapted to the velocity nodes (pressure anti-nodes) of standing sound waves, it is not suitable for the other zones of these waves presenting simultaneous pressure and velocity oscillations. These speed oscillations actually generate a break in the spherical symmetry, the consequences of which need to be analyzed.

2. Spherical liquid drop subjected to a uniform external flow far away

Hill's vortex is used to model the flow within a spherical liquid drop in the presence of relative external flow. [i]

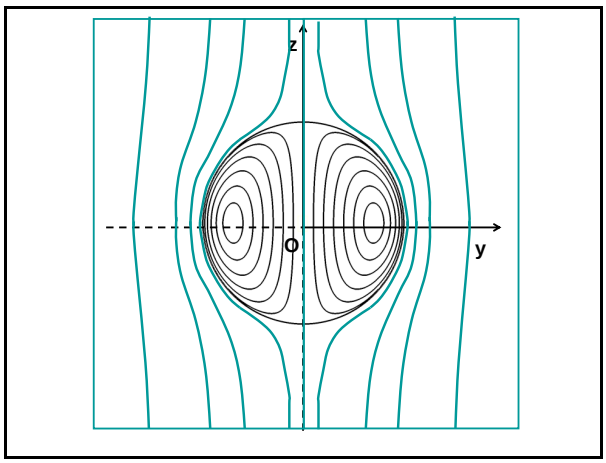

Figure 1. *Liquid drop in the presence of an infinitely uniform flow: shape of the streamlines of the external and internal flows in a plane passing through the axis of symmetry.*

This vortex is *a special case of a stationary motion of revolution of an incompressible inviscid fluid* [ii]*.* It is a rotational motion inside a sphere behaving with an irrotational external flow, so that by choosing suitably the multiplicative constant α of the stream function, the speeds of the two flows are identical to the surface of the sphere [iii].

We first recall the equations of the fluid flow *outside* the sphere of radius *R*, and we will then determine the velocity field of the compatible steady liquid flow[3] *inside* this same sphere[iv].

The stationary flow of a perfect fluid inside a sphere of radius *R* and the flow around this sphere are characteristic examples, shown in figure 1.

2.1. ***Incompressible fluids in spherical coordinates.***

- Understanding the coordinate system

The quantities r, θ,ϕ, are the spherical coordinates, represented in figure 2.

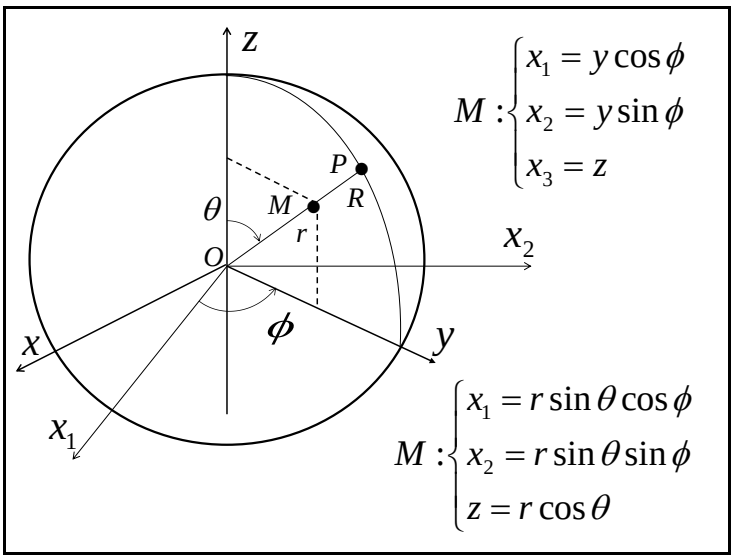

Figure 2. *Definition of the spherical coordinates and representation of a sphere of radius R. The current point M can be inside or outside the considered sphere. P is the point of the half-line OM located at the surface of the sphere.*

In the case of a symmetry around the axis Oz, one works in the plane $\phi = const.$ of figure 2 since the motion is independent of this angle. The basic unit vectors can be defined there.

[3] That is to say with no velocity discontinuity at the interface.

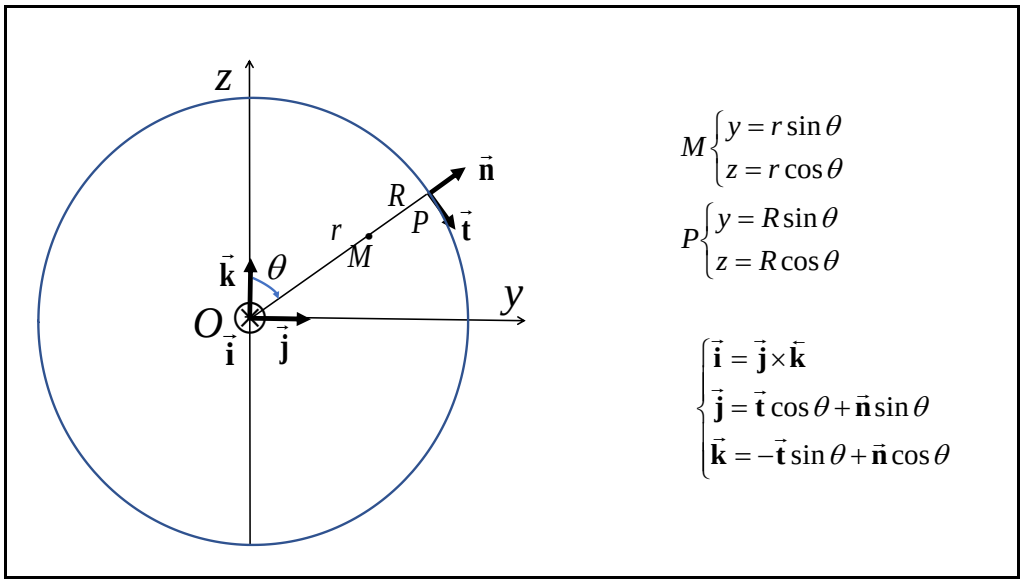

Figure 3. *Definition of the coordinates in the y0z plane containing the axis of symmetry Oz. At the point P of the surface of the sphere of radius R, we define the unit vectors* $\vec{t}$ *tangent and* $\vec{n}$ *normal to the great circle considered. These vectors correspond to the base vectors* $\left(\vec{\mathbf{e}}_\theta, \vec{\mathbf{e}}_r\right)$ *at the point considered.*

- Continuity equation

The continuity equation of an incompressible fluid is written in vectorial notations: $\vec{\nabla}\cdot\vec{\mathbf{v}} = 0$. In expanded form, this gives:

$$\frac{1}{r^2}\frac{\partial}{\partial r}\left(r^2 v_r\right) + \frac{1}{r\sin\theta}\frac{\partial}{\partial\theta}\left(\sin\theta\, v_\theta\right) + \frac{1}{r\sin\theta}\frac{\partial v_\varphi}{\partial\varphi} = 0 \qquad [1]$$

In the case of a symmetry of axis Oz, the motion is identical in each plane containing this axis.

The values of the various quantities of the fluid no longer depend on the angle ϕ. The continuity equation is therefore reduced to: $\frac{1}{r^2}\frac{\partial}{\partial r}\left(r^2 v_r\right) + \frac{1}{r\sin\theta}\frac{\partial}{\partial\theta}\left(\sin\theta\, v_\theta\right) = 0$, and we can then define the velocity field from the stream function ψ as follows:

$$v_r = -\frac{1}{r^2\sin\theta}\frac{\partial\psi}{\partial\theta}, \quad v_\theta = \frac{1}{r\sin\theta}\frac{\partial\psi}{\partial r}, \quad v_\phi = 0 \qquad [2]$$

- Expressions of the stream function in the presence of a sphere

We consider two kinds of flows: a flow irrotational (e) outside the sphere of radius *R*, and a rotational flow (i) with vorticity ω inside the sphere. The flows are connected at any point of their spherical border.

Regarding the vorticity, zero on the outside, it is shown that we have $\omega = 5\alpha_i y$ by virtue of the law of transport of the vortex vector $\vec{\omega}$ into the interior fluid.

In the spherical coordinate system described above, we gets: $r^2 = y^2 + z^2$.

The stream functions ψ_e and ψ_i around and inside the sphere of radius *R,* are expressed as follows[4]:

$$\begin{cases} \psi_e = \alpha_e\, y^2 \left(1 - \dfrac{R^3}{r^3}\right), \text{with } \alpha_e = V_0/2 \text{ for } r \geq R, \text{and} \\ \psi_i = \alpha_i\, y^2 \left(R^2 - r^2\right), \text{with } \alpha_i = -3V_0/4R^2 \text{ for } r \leq R \end{cases} \quad [3]$$

therefore:

$$\begin{cases} \psi_e = \dfrac{V_0}{2}\, y^2 \left(1 - \dfrac{R^3}{r^3}\right) \quad \text{for r} \geq R, \quad \text{and} \\ \psi_i = -\dfrac{3V_0}{4}\, y^2 \left(1 - \dfrac{r^2}{R^2}\right) \quad \text{for } r \leq R \end{cases} \quad [4]$$

In the problem of motion around a stationary sphere of radius *R*, the velocity V_0 is the one at infinity of the external flow: $V_0 = U_\infty$.

The calculations carried out with the stream function are summarized in Table 1. Theys are explicited hereafter.

	Internal flow (Hill vortex) $r \leq R$	External flow $r \geq R$
Stream function	$\psi_i = \alpha_i\, r^2 \sin^2\theta \left(R^2 - r^2\right)$	$\psi_e = \alpha_e\, r^2 \sin^2\theta \left(1 - R^3/r^3\right)$
Velocity $\vec{\mathbf{v}}$	$\begin{cases} v_{ri} = -2\alpha_i \left(R^2 - r^2\right)\cos\theta \\ v_{\theta i} = 2\alpha_i \left(R^2 - 2r^2\right)\sin\theta \end{cases}$	$\begin{cases} v_{re} = -2\alpha_e \left(1 - R^3/r^3\right)\cos\theta \\ v_{\theta e} = 2\alpha_e \left(1 + R^3/2r^3\right)\sin\theta \end{cases}$
Coefficients	$\alpha_i = U_S/2R^2 = -3V_0/4R^2$	$\alpha_e = -U_S/3 = V_0/2$

Table1. *Correspondence between the coefficients for an external flow coming from the negative x with the velocity modulus U_∞. The quantity U_S is the speed at the surface of the sphere at z = 0. This table incorporates the results of section 2.*

2.2. Flow outside the sphere

The steady flow of inviscid fluid outside the sphere is an irrotational flow. Its stream function (Figure 3) is (index *e* for exterior):

$$\psi_e = \alpha_e\, r^2 \sin^2\theta \left(1 - \frac{R^3}{r^3}\right), \quad r \geq R, \quad \alpha_e = \frac{U_\infty}{2} \quad [5]$$

The components of the velocity vector are:

$$v_{re} = -2\alpha_e \left(1 - R^3/r^3\right)\cos\theta, \quad v_{\theta e} = 2\alpha_e \left(1 + R^3/2r^3\right)\sin\theta \quad [6]$$

Its streamlines are represented in figure 4 with:

[4] Ref. iii, p. 312.

$$\bar{z} = z/R,\ \bar{y} = y/R,\ \bar{\psi}_e = 2\psi_e/U_\infty R^2 . \qquad [7]$$

Maximum velocity:

Let us call U_S the value of the speed in $z = 0,\ y = R$, which corresponds to $r = R, \theta = \pi/2$. We find: $U_{Si} = U_{zi} = 2\alpha_i R^2,\ U_{yi} = 0$. If we want U_S to be positive, then we have α to be positive. We then have: $\alpha_i = U_S/2R^2$ and the stream function is written: $U_{Si} = U_{zi} = 2\alpha_i R^2, U_{yi} = 0$. U_S is the maximum value of U at the surface of the sphere.

The velocity vectors of this flow and of the internal flow will be identical at any point on the surface of the sphere if the speed at infinity is suitably chosen: $U_{re}(\infty) = -U_{re}(-\infty) = U_\infty$.

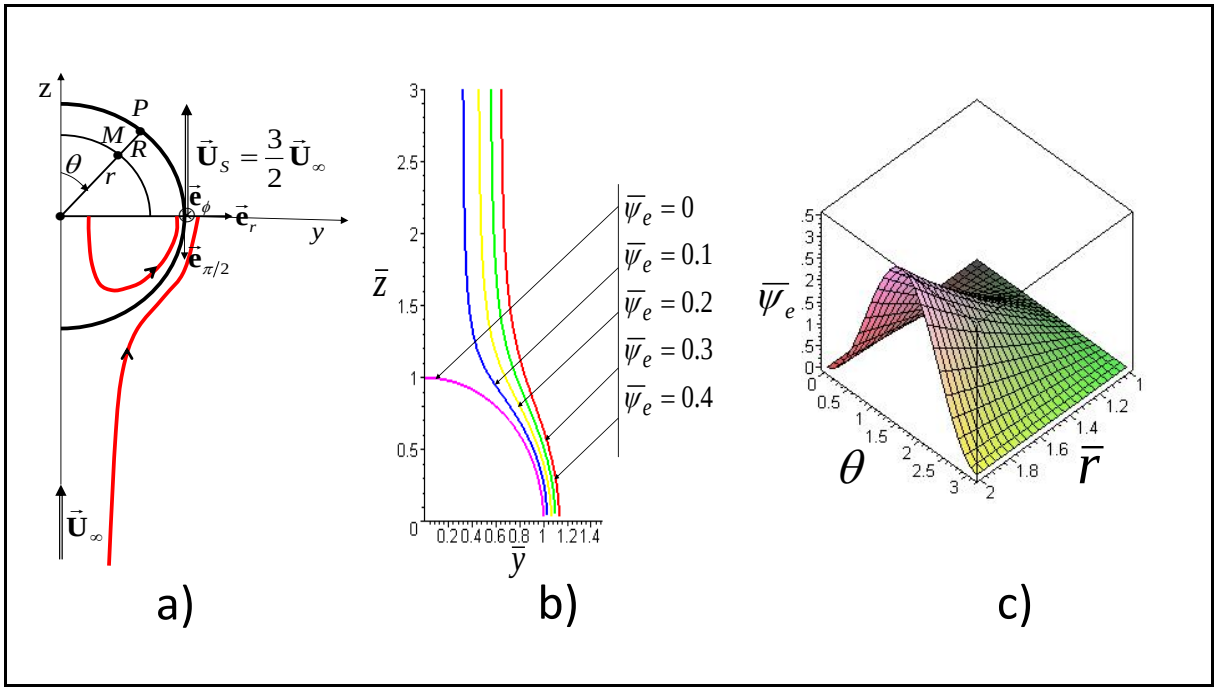

Figure 4. *a) Inner and outer streamlines, speed vectors $\vec{U}_\infty$ at infinity and $\vec{U}_S$ maximum at the surface. b) Streamlines of the flow outside the sphere in the upper quarter plane passing through the axis. $\bar{z} = \bar{z}(\bar{y})$, for different values of the reduced stream function $\bar{\psi}_e = 2\psi_e/U_\infty R^2$. c) Stream function as a function of spherical coordinates θ and reduced radius $\bar{r}$.*

2.3. Flow inside the sphere

- Hill vortex

The stream function of the form:

$$r \le R, \quad \psi_i = \alpha_i r^2 \sin^2\theta\left(R^2 - r^2\right) \qquad [8]$$

corresponds to an internal rotational flow (ref. iii).

Knowing the stream function of the internal flow, we find the following radial and angular components of the velocity vector:

$$v_{ri} = -2\alpha_i\left(R^2 - r^2\right)\cos\theta, \quad v_{\theta i} = 2\alpha_i\left(R^2 - r^2\right)\sin\theta \qquad [9]$$

The results are shown in Figure 5.

Each value of the stream function corresponds to a toric surface. The limit value $\overline{\psi}_i = 0$ is the sphere itself.

The velocity vectors of the external flow are identical to those of the Hill vortex at any point on the surface of the sphere if the constants α_i and α_e are chosen suitably and in relation to the speed at infinity U_∞ [one has : $v_{re}(\infty) = -v_{re}(-\infty) = U_\infty$].

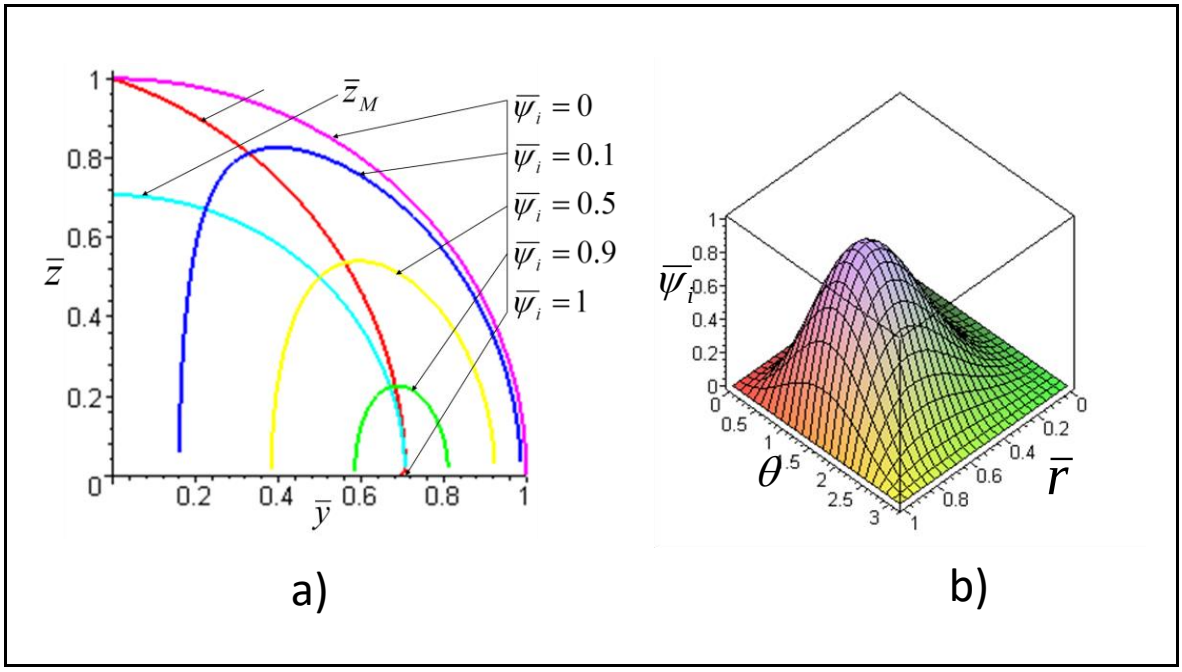

Figure 5. *a) Streamlines calculated in the upper quarter plane passing through the axis.* $\overline{z} = \overline{z}(\overline{y})$, $\overline{y} = y/R$, $\overline{z} = z/R$, *for multiple values of* $\overline{\psi}_i = 4\psi_i/\alpha_i R^4$, $\overline{z}_M(\overline{y})$. *corresponds to the geometrical locus of the points of contact of the straight lines issued from O and tangents to the streamlines. It is a quarter circle of radius* $R\sqrt{2}/2$. *The curve* $\overline{z}_U(\overline{y})$ *is the geometrical locus of the points where the speed is minimum. b) Stream function as a function of spherical coordinates* θ, $\overline{r}$.

One finds in this case:

$$\alpha_i = 3U_\infty/4R^2, \ \alpha_e = -U_\infty/2 \qquad [10]$$

Let us call U_S the value of *the maximum speed at the surface of the sphere*, which occurs in $y = R, z = 0$, which corresponds to: $\theta = \pi/2$. We find: $U_{Si} = 2\alpha_i R^2$. If you

want U_S to be positive, then you have α_i to be positive. We then have: $\alpha_i = U_S / 2R^2$ and the stream function is written:

$$\psi_i = \frac{U_S}{2} r^2 \sin^2\theta \left(R^2 - r^2\right) \qquad [11]$$

We therefore know how to determine the velocity field and the stream surfaces of the flows internal and external to the sphere (ref. iii). It has been shown that then the flows are compatible if $\alpha_i = 3U_\infty / 4R^2$. The maximum speed at the surface of the sphere could then be determined.

- Remark about viscous fluid vortex

The balance equation of the vortex vector in incompressible viscous fluid is written:

$$\partial \vec{\boldsymbol{\omega}} / \partial t + \vec{\nabla} \times \left(\vec{\nabla} \times \vec{\boldsymbol{\omega}}\right) = \nu \, \Delta \vec{\boldsymbol{\omega}} \qquad [12]$$

with, in spherical coordinates:

$$\omega = \frac{1}{2r}\left[\frac{\partial\left(r v_\theta\right)}{\partial r} - \frac{\partial v_r}{\partial \theta}\right] \vec{\mathbf{e}}_\phi$$

<u>In the case of the flow inside the sphere</u>, we find without difficulty for the Hill vortex:

$$\vec{\boldsymbol{\omega}}_i = -5\alpha_i \, r \sin\theta \, \vec{\mathbf{e}}_\phi .$$

The intensity ω_i of the vortex vector is proportional to the distance $y = r\sin\theta$ from the axis of symmetry. The second term of the vortex vector balance is calculated as follows.

We set: $\vec{\mathbf{A}} = \vec{\nabla} \times \vec{\boldsymbol{\omega}}$ and we get:

$A_r = 10\alpha_i r \sin^2\theta \left(R^2 - 2r^2\right)$, $A_\theta = 10\alpha_i r \sin\theta\cos\theta \left(R^2 - r^2\right)$.

We then find: $\vec{\nabla} \times \vec{\mathbf{A}} = \vec{\nabla} \times \left(\vec{\nabla} \times \vec{\boldsymbol{\omega}}\right) = \frac{1}{2r}\left[\frac{\partial\left(r A_\theta\right)}{\partial r} - \frac{\partial A_r}{\partial \theta}\right] \vec{\mathbf{e}}_\varphi = \vec{\mathbf{0}}$. In steady flow: $\frac{\partial \vec{\boldsymbol{\omega}}}{\partial t} = \vec{\mathbf{0}}$. It follows that the term of the second member of the vortex balance equation [12], $\nu \, \Delta \vec{\boldsymbol{\omega}}$ is also zero.

The consequence is that Hill's vortex, a solution of perfect fluid, is also a solution of the equations of viscous fluids.

<u>In the case of external flow</u>, we obviously have $\vec{\boldsymbol{\omega}}_e = \vec{\mathbf{0}}$ since the flow is irrotational.

3. Flows of a spherical liquid drop subjected to an axial thermal gradient

3.1. Presentation of the problem

The effect of an axial temperature field imposed on the internal motions of a liquid spherical drop has been studied by various authors. These movements are caused by the variations in surface tension induced and by the resulting Marangoni effect in viscous fluid.

We can cite in particular Bauer [v,vi,vii]. For mathematical analysis, spherical harmonics are generally used.

In the article by Bauer (1982), a free-floating liquid drop is subjected on its surface to an axial temperature field inducing a thermal convection of Marangoni due to the variation of the surface tension. The stream function and the velocity distribution are determined analytically for the stationary and unsteady temperature fields, by solving the equation verified by the stream function using the associated Legendre functions of the first type. The particular case of a stable linear axial temperature field is evaluated numerically.

We consider the case of axial symmetry *Oz*, the liquid drop being centered in *O*. The equation of continuity of the flow of the supposedly incompressible liquid is written:

$$\frac{1}{r^2}\frac{\partial}{\partial r}\left(r^2 u\right)+\frac{1}{r\sin\theta}\frac{\partial}{\partial\theta}\left(v\sin\theta\right)=0$$

where u is the radial velocity and v the angular velocity[5]. We can therefore introduce the stream function ψ such that:

$$u=-\frac{1}{r^2\sin\theta}\frac{\partial\psi}{\partial\theta},\ v=\frac{1}{r\sin\theta}\frac{\partial\psi}{\partial r} \qquad [13]$$

By removing the pressure from the unsteady momentum equations, and defining the operator:

$$\overline{\Delta}=\frac{\partial^2}{\partial t^2}+\frac{\sin\theta}{r^2}\frac{\partial}{\partial\theta}\left(\frac{1}{\sin\theta}\frac{\partial}{\partial\theta}\right) \qquad [14]$$

It comes:

$$\overline{\Delta}\left[\overline{\Delta}\psi-\frac{1}{\nu}\frac{\partial\overline{\psi}}{\partial t}\right]=0 \qquad [15]$$

H.F. Bauer first deals with *the stationary case* by assuming constant the derivative of the surface tension σ with respect to the temperature *T*.

This temperature develops in a series of Legendre polynomials as follows:

$$T_0+T_1\ f_0(\xi)=\sum_{n=0}^{\infty}\alpha_n\ P_n(\xi) \qquad [16]$$

With $\xi=\cos\theta$ and the relation of orthogonality:

$$\int_{\xi=-1}^{+1}P_m(\xi)P_n(\xi)d\xi=\begin{cases}0 \quad \text{for} \quad m\neq n\\ \dfrac{2}{2n+1}\text{for} \quad m=n\end{cases} \qquad [17]$$

The temperature distribution inside the spherical drop is given by:

$$T(r,\theta)=\sum_{n=0}^{\infty}\alpha_n\left(\frac{r}{a}\right)^n P_n(\cos\theta) \qquad [18]$$

[5] u and v were noted v_r and v_θ in section 2.1.2

with coefficients α_n checking:

$$\alpha_n = \left[T_0 \int_{-1}^{+1} P_n(\xi) d\xi + T_1 \int_{-1}^{+1} f_0(\xi) P_n(\xi) d\xi \right] \frac{2n+1}{2} \qquad [19]$$

In the case of a temperature at the surface of the form $T = T_0 + T_1 R\cos\theta$, we have

$\alpha_0 = T_0, \quad \alpha_1 = T_1 R, \quad \alpha_n = 0$ for $n > 1$

The temperature distribution inside the drop is then of the form $T(r,\theta) = T_0 + T_1 r\cos\theta$, with :

$\int_{-1}^{+1} P_0(\xi) d\xi = 2$ and $\int_{-1}^{+1} P_n(\xi) d\xi = 0$ for n>1, and $\int_{-1}^{+1} \xi P_n(\xi) d\xi = \begin{cases} 2/3 & \text{for} \quad n = 1 \\ 0 & \text{for} \quad n > 1 \end{cases}$

One thus solves the equation $\overline{\Delta}\,\overline{\Delta}\psi = 0$ with the boundary condition of interface in $r = R$:

$$\tau_{r\theta} = \mu \left[r \frac{\partial}{\partial r}\left(\frac{v}{r}\right) + \frac{1}{r}\frac{\partial u}{\partial \theta} \right] = \frac{T_1}{a} \left| \frac{d\sigma}{dT} \right| f'_0(\xi) \sin\theta \qquad [20]$$

and the fluxes cancellation conditions:

$$\int_0^{2\pi} \int_0^{a} v \sin\theta_0 \, r \, d\varphi \, dr = 0 \text{, and } \int_0^{\pi} \int_0^{2\pi} u_{r=r_0} r_0^2 \sin\theta \, d\varphi \, d\theta = 0 \qquad [21]$$

In the case of the linear axial temperature: $T = T_0 + T_1 R\cos\theta$, we find the stream function

$$\psi(r,\theta) = -\frac{T_1 R^3}{6\mu} \left| \frac{d\sigma}{dT} \right| \left[\left(\frac{r}{R}\right)^2 - \left(\frac{r}{R}\right)^4 \right] sin^2\,\theta \qquad [22]$$

which corresponds to the case of the Hill vortex in section 2.2.

Bauer also solves the problem in the case of an axial field of any stationary temperature, or with a periodic dependence in time.

3.2. Thermo-capillary Hill vortex

In the study by Bauer (1982), we notice that the solution obtained in the case of a constant axial thermal gradient was a Hill vortex with the same axis. [6]

The result can be obtained directly as follows. Consider a spherical drop of liquid whose surface is a phase separation of capillary tension σ. We assume that this surface tension is a linear function of the temperature:

$$\sigma = \sigma_0 + \sigma_T (T - T_0) \qquad [23]$$

The motion of the liquid is organized in a Hill vortex, but if we assume that the outer fluid is inviscid and incompressible, it is at rest.

---

[6] Unlike section 2, the spherical drop is not in the presence of a well-defined external flow. This does not have a great importance if one neglects the interaction between the drop and the possible motions in its exterior.

We can ask ourselves the following question: Which temperature field is capable of generating a Hill vortex as a result of the surface motion of the drop by thermo-capillary effect?

To answer this question, we establish the conditions of equilibrium to be verified between the capillary forces and the viscous forces at the surface of the sphere.

At point M, the velocity vector is (Figures 2 and 3, with $U_\infty = V_0$ in the case of section 2):

$$\vec{\mathbf{v}}_i = \frac{3V_0}{2}\frac{y}{R^2}\left(y\,\vec{\mathbf{i}} - z\,\vec{\mathbf{k}}\right) = \frac{3V_0}{2}\left[\frac{r^2}{R^2}\,\vec{\mathbf{t}}\sin\theta + \left(\frac{r^2}{R^2} - 1\right)\vec{\mathbf{n}}\cos\theta\right] = \frac{3V_0}{2}\left(v_t\,\vec{\mathbf{t}} + v_n\,\vec{\mathbf{n}}\right) \qquad [24]$$

In *P*, that is to say for $r = R$, we have: $\vec{\mathbf{v}} = \vec{\mathbf{U}} = -2\alpha_i R^2 \sin\theta\,\vec{\mathbf{e}}_\theta = \frac{3V_0}{2}\,\vec{\mathbf{t}}\sin\theta$.

The balance of forces at a point on the capillary surface of the spherical drop involves the calculation of the tangential strain rate:

$$\varepsilon_{tn} = \frac{1}{2}\left(r\frac{\partial\left(U_t/r\right)}{\partial r} + \frac{1}{r}\frac{\partial U_n}{\partial\theta}\right) \qquad [25]$$

which makes it possible[7] to express the tangential stress $\tau_{tn} = 2\,\mu\,\varepsilon_{tn}$.

One has: $\frac{U_\theta}{r} = \frac{2\alpha_i}{r}\left(R^2 - 2r^2\right)\sin\theta$, $U_r = 2\alpha_i\left(r^2 - R^2\right)\cos\theta$, therefore:

$$\tau_{\theta r} = \tau_{r\theta} = 6\,\mu\,R\,\alpha_i\sin\theta \qquad [26]$$

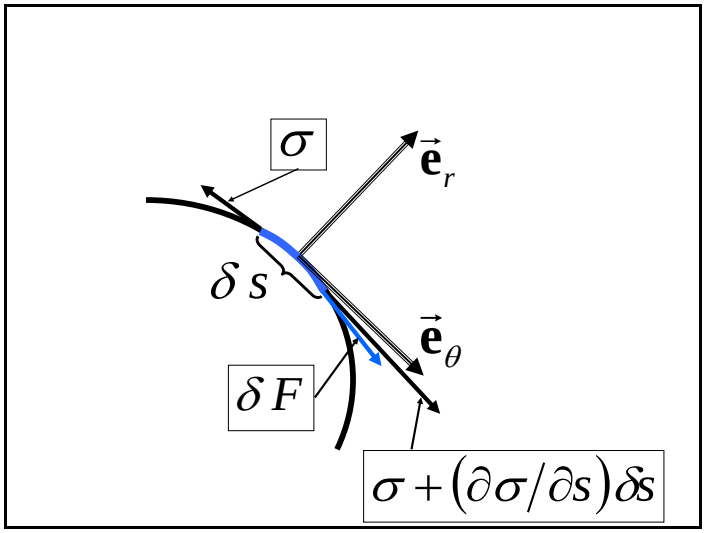

Figure 6. *Forces at the surface of the liquid.* $\delta s = R\,\delta\theta$, *F: viscous friction force.*

This tangential stress is equal to: $\frac{\partial\sigma}{\partial s} = \frac{1}{R}\frac{\partial\sigma}{\partial\theta} = \frac{\sigma_T}{R}\frac{\partial T}{\partial\theta}$ (Figure 6).

[7] The surface forces are calculated from the speed field of the Hill vortex by introducing a viscosity, whereas this vortex is an inviscid fluid flow. This is not contradictory if we admit that it is a local influence and that the bulk of the flow is changed very little.

It follows that $\frac{\partial T}{\partial \theta} = \frac{4\mu R^2 \alpha_i}{\sigma_T} \sin\theta$, either: $T = T_0 - \frac{4\mu R^2 \alpha_i}{\sigma_T} \cos\theta$, or again:

$$T = T_0 - \frac{4\mu R \alpha_i}{\sigma_T} z \qquad [27]$$

There is a constant gradient temperature field.
We can therefore give the following result:

A spherical liquid drop of constant density, subjected to a uniform and constant temperature gradient $\vec{\mathbf{G}} = \vec{\nabla} T$ *in an atmosphere at rest, is animated by the internal motion corresponding to the Hill vortex whose velocity of maximum intensity is oriented in the opposite direction to* $\vec{\mathbf{G}}$ *(Figure 7):* $U_{SG} = G\sigma_T R/2\mu$, *G being the thermal gradient* $G = dT/dz$. *Then we have:*

$$U_{\max} = 3V_0/2 = G\sigma_T R/2\mu \qquad [28]$$

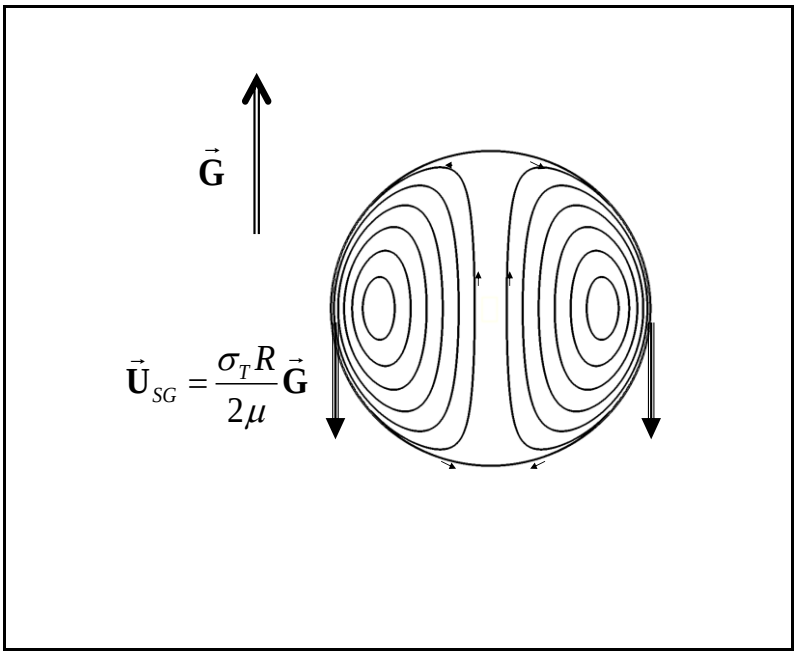

Figure 7. *Hill vortex generated by a thermal gradient.*

3.3. Other thermo-capillary flows

As indicated at the beginning of section 3.1, Bauer also deals with instabilities in cases other than that of the constant axial thermal gradient.

In his 1985 paper, Bauer (ref.vi) studies the combined effects of Marangoni convection induced by a temperature gradient imposed on the free surface of a liquid sphere and natural convection from the residual microgravity field existing in an orbiting space laboratory[viii]. The case of a constant and linearly dependent axial residual gravity field was considered, for which the Stokes equation in the Boussinesq approximation was solved.

A dynamic Bond number derived from the ratio of the Grashof number, and the Reynolds number based on the Marangoni flow is introduced. It makes it possible to determine the predominance of the Marangoni effect if $Bo \to 0$ or of natural convection if $Bo \to \infty$.

The combined effects of Marangoni and natural convection are then studied. Streamlines, radial and angular velocity distributions have been obtained analytically. On the other hand, the isotherms are presented for different temperature distributions imposed on the free surface of the liquid sphere.

The dynamic Bond number introduced is by definition:

$$\tilde{Bo} = \rho g \beta R^2 / |\sigma_T| \qquad [29]$$

It compares the buoyancy force to the surface tension.

The main gravitational influence is due to the residual acceleration normal to the orbital path, in the plane of the orbit. It is created by the centrifugal acceleration of the space station in circular orbit and the acceleration of Newton.

When *g* is constant, we write $g = g_0$; for *g* variable, we have $g = \Omega_0^2 R$ where Ω_0 is the angular velocity of the center of mass around the center of the earth. Equations [12] to [14] still apply, but equation [15] is replaced by

$$\bar{\Delta}\left[\bar{\Delta}\psi - \frac{1}{\nu}\frac{\partial \bar{\psi}}{\partial t}\right] = -\frac{3\Omega_0^2 \beta}{\nu}\left[r^2 \frac{\partial T}{\partial r}\sin\theta\cos\theta + r\frac{\partial T}{\partial \theta}\cos^2\theta\right]\sin\theta \qquad [30]$$

where β is the coefficient of thermal expansion of the liquid.

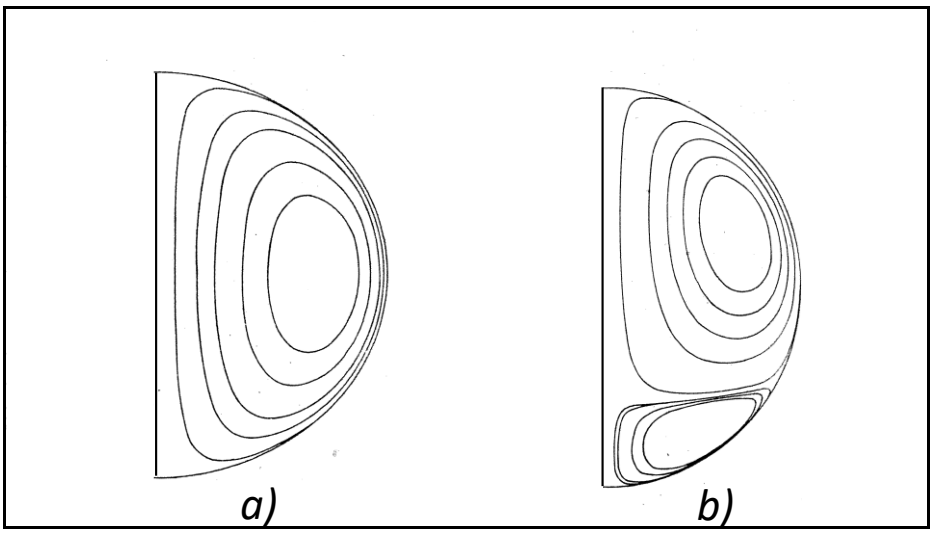

Figure 8. *Streamlines of vortex rings in the presence of a variable gravity field (redrawn from Bauer 1985): a) for a linear temperature field and b) quadratic.*

We then use the recurrence formulas of Legendre functions. The calculations lead to expressions of the stream function $\psi(r,\theta)$ and of the components of the velocity vector $u(r,\theta), v(r,\theta)$ according to series expansions of $P_n^0(\cos\theta)$, and $P_n^1(\cos\theta)$.

The constants involved in these expressions are to be determined according to the boundary conditions at the surface of the liquid sphere.

In the absence of capillary effects, natural convection is obtained due to the residual gravity present at the location of the space station where the drop is located. We must then distinguish the case where liquid is in a rigid container from the case of the free surface $\widetilde{B}_0 \to \infty$, where we can neglect the thermo-capillary effects.

One also solves the situations where the internal motions of the drop of thermo-capillary origin are important, and we can thus predict the effects of residual gravity on these movements.

With regard to the field of gravity two situations are examined numerically: constant micro-gravity and linearly varying micro-gravity.

As for the field of temperature the field is linear axisymmetric $T = T_0 + T_1 \cos\theta$, or mixed linear-quadratic $T = T_0 + T_1 \cos\theta + T_2 \cos^2\theta$.

Results of the calculations carried out show in Fig. 8 the possibility of notable differences with Hill's vortices. Two-ring configurations of stream surfaces are observed (figures redrawn from the 1985 Bauer article) with a variable residual gravity field and quadratic temperature fields for $T_2/T_1 = 2$ with $\widetilde{Bo} = 0, 10, 100$.

Another figure of the cited article also shows a case with two tore surfaces with a constant residual gravity field, the same quadratic temperature field and $\widetilde{Bo} == 10$.

4. Conclusion

We have presented Hill's vortex as a structure that can appear inside liquid drops under two circumstances: infinitely uniform external fluid flow, thermal gradient along an axial direction. In both cases the speed of the fluid at the level of the surface of the drop is found to be proportional to the distance from the axis of symmetry.

The physical assumptions were:

– The sphericity of the drop of constant radius

– The liquid: incompressible, expandable, or not, viscous but animated by a rotational motion of inviscid fluid in stationary regime

– The external fluid: at rest or animated by a uniform motion far away, inviscid irrotational or locally viscous

– Concerning the external liquid fluid interface:

- o Simple contact surface or sliding surface
- o Identity of speeds: fluids-surface or only liquid-surface
- o With or without surface tension depending on the temperature. We took care to situate the case of the Hill vortex as a particular case of analysis by series of Legendre functions.

Outlook:

On the Hill vortex, it will be necessary to conclude on the birth and dissipation of this vortex by providing characteristic times [ix, x].

On the Marangoni instability in a drop subjected to a radial thermal field with spherical symmetry, we will have to refine our formulation of the problem in spherical coordinates using the articles of Hoefsloot et al. [xi, xii].

It would be interesting to study the effect of the thermo-capillary vortex on the evaporation of the drop [xiii, xiv], in particular in the presence of thermal radiation [xv] or acoustic excitation as we have done with other phenomena [xvi].

Researchers are already interested in pursuing investigations on the subject[8].

[8] In particular at the University of Lomé (Togo), and at the University of Abomey-Calavi (Benin).

Appendix

A1. Possible motions into a liquid drop.

In the absence of external flow, an internal thermal gradient in the liquid can cause internal motions for two reasons. At first, because the resulting density gradients lead to natural convection in the presence of gravity. Secondly, even without gravity, because the surface tension gradients caused by the surface thermal gradients are at the origin of the Marangoni effect which does not depend on gravity.

We know that these phenomena can come into play even in configurations having in principle solutions at rest, beyond instability thresholds. This is the case of the following two instabilities appearing classically in a flat horizontal layer configuration:

- *The Rayleigh-Bénard instability* which appears in a liquid layer of thickness *h* heated from below in the presence of gravity[xvii], above a critical value of the Rayleigh number. Recall that the Rayleigh number is defined by $Ra = Gr_{Th}\,\mathrm{Pr}$ where we find the thermal Grashov number $Gr_{Th} = \Delta\rho\, g\, L^3 / \rho\nu^2$ and the Prandtl number $\mathrm{Pr} = \nu/\kappa$. Finally, $Ra = \alpha G\, g\, h^4 / \kappa\nu$: with *G* thermal gradient of reference, α coefficient of dilation . For a layer with two free boundaries, the critical Rayleigh number for which instabilities appear is equal to 657.511 for a reduced wavenumber of 2.2214. [9]
- *The Bénard-Marangoni instability* also appears in a liquid layer with transverse thermal gradient presenting capillary surfaces. It is due to the sensitivity of surface tension to temperature [xviii, xix].

In the case of the drop, the curved configuration certainly involves both natural convection and the thermocapillary effect, which importance should be evaluated by using specific numbers of Rayleigh and Marangoni.

The presence of an external flow in the reference configuration of the drop causes internal motions. Outflow may be due to natural convection in the gas phase (we can think of acoustic agitation), but the external flow can also be caused by the difference between internal speeds of the spray for the drop and for the gas phase.

The flow in a spherical liquid drop in the presence of relative flow can be modeled by a Hill vortex [xx], [xxi]. It is a three-dimensional flow of revolution the stream functions are well defined in spherical coordinates by the relations given in section 2.

The following dimensionless numbers are used to evaluate and compare fluxes:

- *the Peclet number of the liquid,* which compares convection and heat conduction, $Pe_L = Re_L\, Pr_L$ is the product of the Reynolds number and the Prandtl number. Therefore, it can be written: $Pe_L = 2\rho_L U_S R/\kappa_L$, with $\kappa_L = k_L/\rho_L\, c_L$ thermal diffusivity.

- *the Nusselt number of the liquid* which involves the convection coefficient α and the thermal conductivity: $Nu = \alpha L/\kappa$. We then have $Nu_L = \chi\, Nu_L(0)$, where $Nu_L(0) = 6.58$ corresponds to the solid sphere. The heat conduction factor χ is a Peclet function: $\chi = 1.86 + 0.86\, th\left[2.245 log_{10}\left(Pe_L/30\right)\right]$. The figure A1 gives the curve $\chi(Pe_L)$.

[9] Note that the case of the liquid sphere treated by Chandrasekhar corresponds to a central force field (case of the terrestrial globe) is very different. Nevertheless, the Rayleigh number can give valuable indications of possible convection.

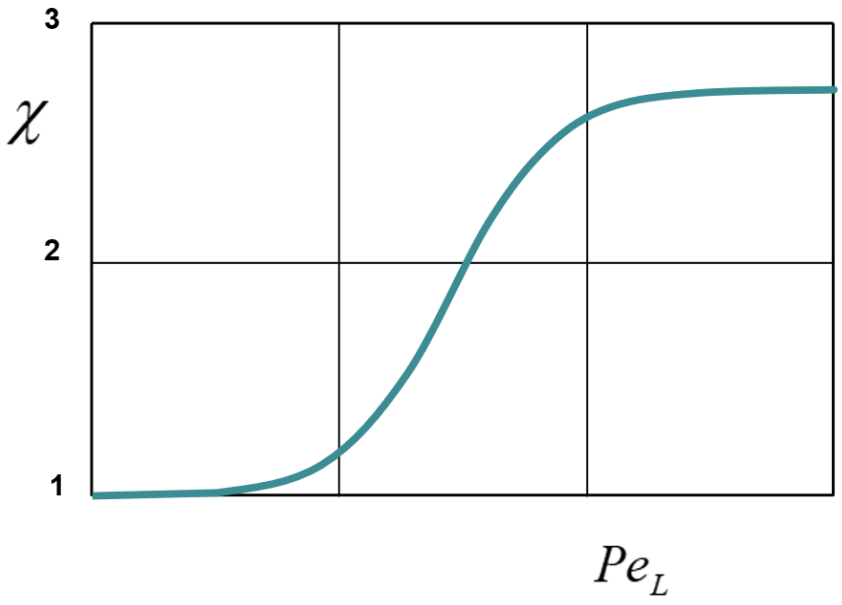

Figure A1. *Effective heat conduction factor depending on the Peclet number of the liquid* [xxii]

- On the side of the *gaseous phase*, the *modified Nusselt* $Nu*$ *and Sherwood* $Sh*$ *numbers* are used to characterize the transfers towards the drop. We thus have then for the mass flow rate of vaporization of the droplets of radius r_S:

$\dot{M}=4\pi\frac{k}{c_p}r_S Nu^* ln(1+B_T)$, with $B_T = c_p(T_C - T_S)/(\ell + Q_L/\dot{M})$, the Spalding thermal coefficient, and $\dot{M} = 2\pi\rho D r_S Sh^* \ln(1+B_M)$, with the Spalding mass diffusion coefficient $B_M = (Y_{FS} - Y_{FC})/(1-Y_{FS})$.

In these equations, we have *k* for the conduction coefficient, c_p specific heat at constant pressure, T_C and T_S the absolute temperatures respectively far away the droplet an at the surface of the drop, ℓ the latent heat and Q_L the heat flux to the drop coming from outside, Y_j

The mass fraction of the species *j*, respectively

Nusselt and Sherwood numbers are modified to account for evaporation as follows:

$$Nu^* = 2 + \frac{0.6\,Re^{1/2}\,Pr^{1/3}\,B_T}{(1+B_T)^{0.7}\,ln(1+B_T)}, \text{ avec } B_T = c_p(T_C - T_S)/(\ell + Q_L/\dot{M}), \text{ and :}$$

$$Sh^* = 2 + \frac{0.6\,Re^{1/2}\,Sc^{1/3}\,B_M}{(1+B_M)^{0.7}\,ln(1+B_M)}, \text{ avec } B_M = (Y_{FS} - Y_{FC})/(1-Y_{FS}).$$

A2. Acoustic excitation in a rocket engine

The acoustic excitations in a rocket engine can give rise to standing waves of pressure or velocity depending on the position considered. The diagrams in the figure A2 show the

situations of acoustic excitation by plane parallel emitters. In the case of the anti-nodes of speed, it will be necessary to specify the relative direction of the excitation in speed compared to the flow: parallel, perpendicular, specified angle.

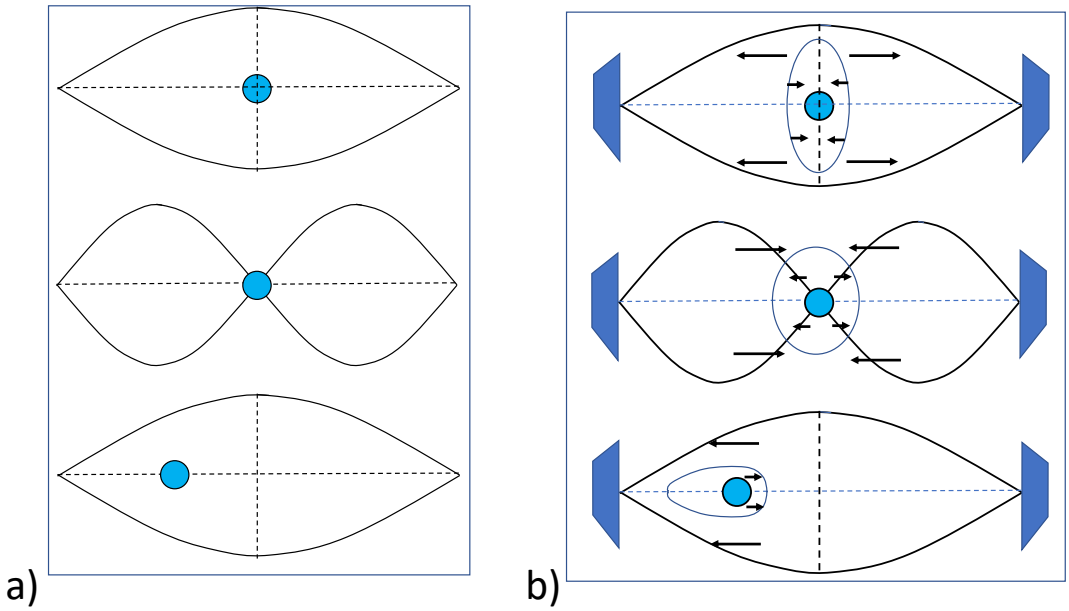

Figure A2. *Thermo-acoustic streaming pattern. In this figure, the curves represent the velocity profile of the acoustic wave produced by the motor.* ***a)*** *The spherical liquid droplet*[10] *can be in a velocity anti-node (top), i.e. in a pressure node. Its position can also be a speed node (in the middle), i.e., a pressure anti-node. It can also undergo the effects of velocity and pressure (bottom) of the standing acoustic wave.* ***b)*** *In the case studied by Tanabe et all*[xxiii]*, another phenomenon is observed. When a droplet burns at anti-node (upper case), fuel vapour comes back to concentrate on the anti-node plane and the burned gas flows towards the node. At node (middle case), flows in opposite direction can be expected. In the middle of node and anti-node (lowercase), a natural convection-like flow occurs.*

In our studies, we are interested in liquid evaporating droplets flowing inside a rocket engine, and we assume that the flame surrounds a population of these droplets. A mean drop of this population will be considered.

A3. The mean vaporizing droplet, continuously fed by a point source placed at its centre.

In the present theory, we admit that the history of the droplets moving in a rocket engine can be described by a single mean droplet. This vaporizing liquid droplet submitted to the acoustic oscillations coming from the engine, is continuously fed, at its centre, by a liquid flow that compensate exactly the loss of mass by evaporation. This feeding mass rate is equal to this which would be vaporized during the stabilized unperturbed evolution.

The mean droplet is supposed to be situated at a velocity node such as represented in figure A2 (in the middle). Therefore, we only consider pressure perturbation and associate

[10] In our studies, we are interested in liquid drops, and we assume that the flame surrounds a bundle of many evaporating drops. In the Heidmann configuration, the considered droplet is a mean one which represents the whole drops moving in the combustion engine.

(but not speed perturbations) [xxiv]. In addition, the study is limited to small perturbations, what permits then linearized calculations with several possible hypotheses concerning the feeding mode[xxv].

Applying this method, we find generally approximate analytic expressions for:

- The response factor, which permit the determination of sound frequency limits between stable and unstable regions.
- The temperature field inside the droplet.

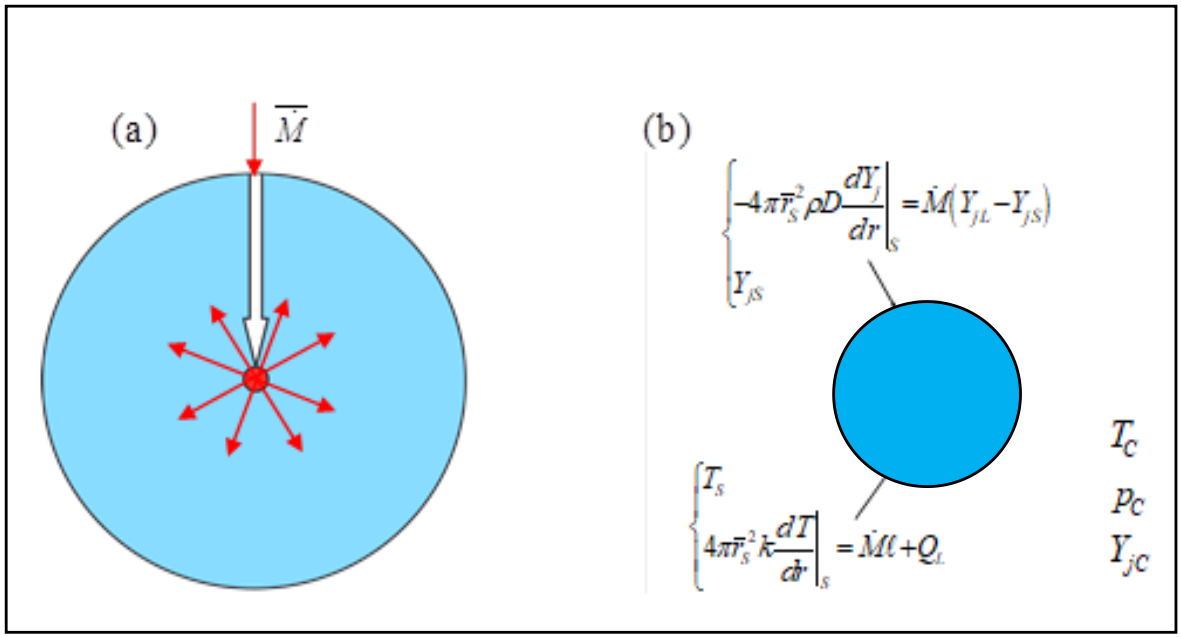

Figure A3. *a) The mean vaporizing droplet, continuously fed by a point source placed at its centre. b) Boundary conditions for the supplied droplet.*

The geometrical configuration is given in Figure A3a, and the boundary conditions far away and at the droplet surface appear in Figure A3b.

In the equations $\dot{M}, \overline{\dot{M}}, T, Y_j, p, \rho, r, \bar{r}_S, D, k, \ell, Q_L$ are respectively the instantaneous evaporating mass, the average feeding mass flow rate, the values of temperature, species mass fraction, pressure, density, radial coordinate, stabilized droplet radius, diffusion coefficient, heat conduction, latent heat, heat transferred from outside into the droplet. Indexes *L*, *C* and *S* are used for the liquid phase, the combustion chambre, and the droplet surface.

Simple results are obtained with an adiabatic feeding at the centre and neglecting the motion inside the droplet. The obtain results are of the form:

$$N = \alpha\Re\left\{\frac{iu}{1+iu}\,\frac{A+\theta E(u,\theta)}{B-\theta E(u,\theta)}\right\}$$

for the response coefficient, and

$$X = \Re\left\{\frac{A+B}{B-\theta E(u,\theta)}\,\frac{\sinh\left[(1+i)\sqrt{3u/2\theta}\,\xi\right]}{\sinh\left[(1+i)\sqrt{3u/2\theta}\right]}\,e^{\frac{iu}{3}\tau}\right\}$$

for the reduced temperature perturbation inside the droplet.

In these formulae, constants *A, B,* and α depends on the reference state thermal and chemical quantities. $u = 3\omega\bar{\tau}_v, \omega$ being the pulsation of the sound wave is a reduced frequency , θ is the inverse of the Peclet number, ξ, τ are reduced radius and time. We have:

$$\begin{cases} \theta = 9\kappa_L \bar{\tau}_v / \bar{r}_S^2 = \bar{\tau}_v / \tilde{\tau}_T \\ E(u,\theta) = 1 - (1+i)\sqrt{3u/2\theta}\coth\left[(1+i)\sqrt{3u/2\theta}\right] \end{cases}$$

where $\bar{\tau}_v, \tilde{\tau}_T$ are characteristic times for mass and heat exchange, and κ_L is the heat diffusion coefficient of the liquid.

An example of the obtained results is presented in Figure A4. We observe in particular that increasing θ (i.e., decreasing *Pe* $= \tilde{\tau}_T / \bar{\tau}_v$) lead to enlarge the unstable frequency domain ($N/\alpha > 0$). We see too that, for a given value of θ, a frequency increasing reduces the penetration of the thermal wave inside the drop.

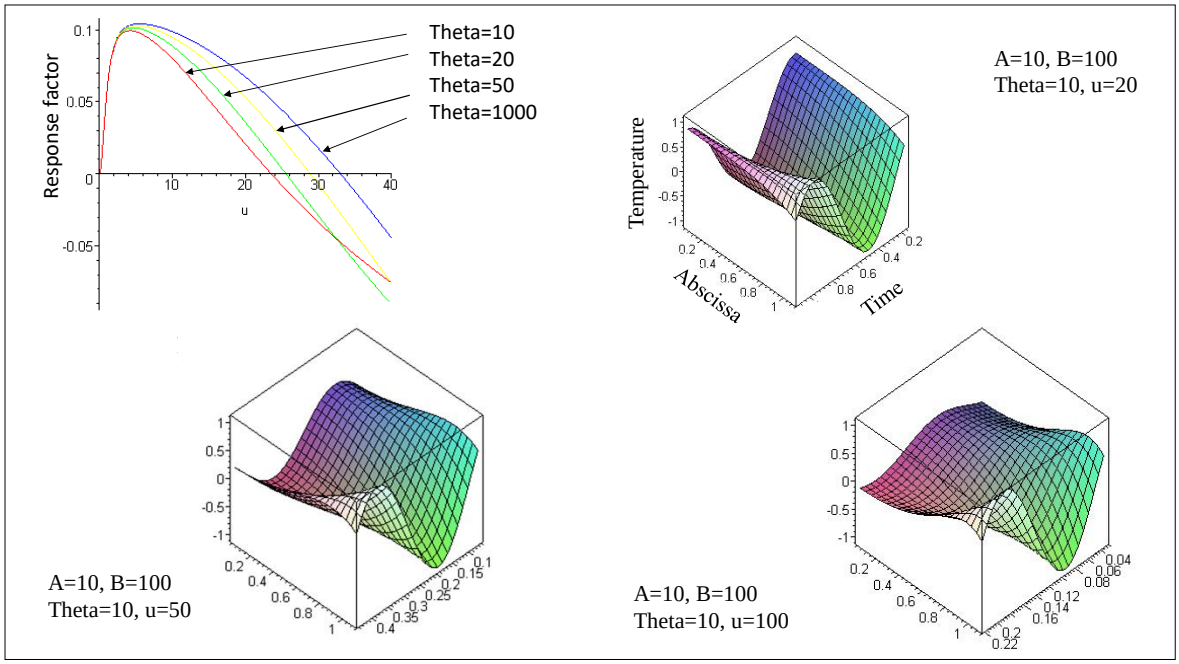

Figure A4. *Spherical drop with adiabatic feeding regime for A=10, B=10. The reduced response factor* N/α *as a function of u for several values of theta. The reduced temperature perturbation as a function of space and time for,* θ *=10 and three values of the sound reduced frequency u.*

The case of an isothermal injection in place of the previous adiabaticity was also studied.

An extension of this study was made introducing a finite exchange injection coefficient at the centre of the drop.

We are interested to extend our research about the mean vaporizing droplet theory to the case of velocity steady acoustic waves. The present paper is a first step.

A4. Effects of turbulence

Turbulence can significantly alter exchanges through mixing. The results will be different depending on whether it is a micro-mix or a macro-mix.

There is generally a distribution of turbulence scales as shown in the figure's *Kolmogorov diagram* valid for a one-dimensional turbulent energy spectrum $E_1(k_1)$ (energy of velocity fluctuations per unit mass and wavenumber), showing the universality $(k_1/k_d)^{-5/3}$ of Kolmogorov's law valid in the inertial zone.

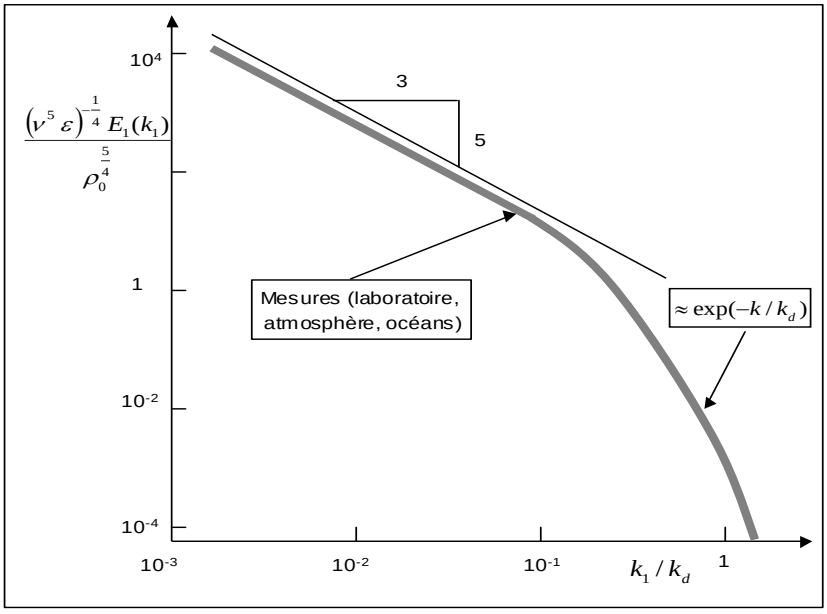

Figure 9. Kolmogorov diagram k_d is the Kolmogorov wave number $k_d = (\bar{\varepsilon}/\nu^3)^{1/4}$ where $\bar{\varepsilon}$ is the rate of energy produced per unit mass in the large scales, equal by assumption to the rate of energy dissipated by viscosity in the small scales.

The *coupling between turbulence and combustion* is complex and is still the subject of numerous investigations. The interaction between evaporating drop and turbulence is also complex. It must be determined whether the size of the drops allows a direct interaction and also whether the gas transfer coefficients are modified.

In the case of evaporating drops, an evaporation time and a mixing time are defined, which are compared to the chemical time[11]:

- the evaporation time is deduced from the law "in d2" which is written: $d^2 = d_0^2 - K t$. We therefore find: $\tau_{vap} = \bar{d}_0^{\,2}/K$ where $\bar{d}_0$ is the mean diameter of the drops (Sauter diameter).

- the mixing time $\tau_{mix} = D/U_{ref}$ is defined by means of the relation , where the outlet diameter *D* of the injector characterizes the large scales of the turbulence and where the reference speed U_{ref} is

11 Delabroy, O., Lacas, F., Labegorre, B., Samaniego, J.-M. (1998): "Paramètres de similitude pour la convection diphasique", *Revue Générale de Thermique*, **37**, 934-953.

defined from the total momentum M_0 of the jet according to identity: $M_0 = \frac{\pi}{4} \rho_{moy} D^2 U_{ref}{}^2$. We therefore find $\tau_{mix} = \frac{\pi^{1/2}}{2} \rho_{moy}{}^{1/2} D^2 M_0{}^{-1/2}$

- Chemical time τ_{ch} also intervenes in this theory, the authors defining it for a premixed flame: $\tau_{ch} = \mathcal{D}/s_l$ ratio of the diffusion coefficient to the combustion rate of the adiabatic flat flame.

- Apparently the small scales of the turbulence do not intervene in this theory. Nevertheless, the ratio of the average diameter of the drops to the outlet diameter of the injector is considered.

The following reports are defined: $\Delta_1 = L_{liq}/L_{ent}$, $\Delta_2 = \tau_{mix}/\tau_{ch}$, $\Delta_3 = \tau_{vap}/\tau_{ch}$, $\Delta_4 = \bar{d}_0/D$. The wavelengths should also be compared with those of the exciting vibrations of the engine. We have seen that in rocket engines, the period $T = 2\pi/\omega$ was of the same order as the heat transfer time $\bar{\tau}_T$, which suggests the existence of coupling and in fact justifies our studies.

References

[i] Abramzon, B. & Sirignano, W. A. : Droplet vaporization model for spray combustion calculations, *Int. J. Heat Mass Transfer*, **32**, Nº 9, 1605-1618, 1989. DOI: 10.1016/0017-9310(89)90043-4.

[ii] Lamb, H.: *Hydrodynamics*, Cambridge University Press, Cambridge, 1945.

[iii] Germain, P. : *Mécanique*, t. I, Ellipses, Ecole Polytechnique, Palaiseau, 1986.

[iv] Prud'homme, R., *Flows and chemical reactions*, WILEY / ISTE, 2012 ISBN 978-1-84821-425-5.

http://www.iste.co.uk/index.php?f=a&ACTION=View&id=506

[v] Bauer, H.F. : Marangoni convection in a freely floating liquid sphere due to axial temperature field. *Ing. Arch.*, **52** , 263-273, 1982.

[vi] Bauer, H.F. : Combined residual natural and Marangoni convection in a liquid sphere subjected to a constant and variable micro-gravity field. Zamm Z. angew. Math. Mech. 65 10, 461-470, 1985.

[vii] Bauer, H.F.& Eidel, W. : Marangoni convection in a spherical liquid system. *Acta Astronautica*, **15,** 275-290, 1987.

[viii] Lefebvre D., Microgravité dans l'ISS, *TangenteX.com* septembre 2018
http://www.tangentex.com/Microgravite.htm

[ix] Gharib M., Rambod E., Shariff K.: A universal time scale for vortex ring formation. J. Fluid Mech., 360:121–140, 1998.

[x] Chung, J.N.: The motion of particles inside a droplet. Transactions of the ASME, **104**, 438-445, August 1982.

[xi] Hoefsloot, H.C.J., Hoostraten, H.W., Janssen, L.P.B.M.: Marangoni instability in a confined between two concentric spherical surfaces liquid layer under zero-gravity conditions. Applied Scientific research, 47, 357-377 (1990).

[xii] Hoefsloot, H.C.J., Hoostraten, H.W., Janssen, L.P.B.M., Knobbe, J.W.: Grows factors for Marangoni instability in a spherical liquid layer under zero-gravity conditions. Applied Scientific research, **49**, 161-173, Kluwer Academic Publishers (1992).

[xiii] Shih, A.T., Megaridis, C.M.: Suspended droplet evaporation modeling in a laminar convective environment. *Combustion and Flame*, **102**: 256-270, 1995.

[xiv] Shih, A.T., Megaridis, C.M.: Thermocapillary flow effects on convective droplet evaporation. *Int. J. Heat Mass Transfer*, **39**, N°2, pp. 247-257, 1996.

[xv] Niazmand, H., Ambarsooz, M., Effect of slip and Marangoni convection on single fuel droplet heat-up in the presence of thermal radiation. ICHEC 2009, Kish Island, I.R. Iran.

[xvi] Mauriot, Y., Prud'homme, R., Assessment of evaporation equilibrium and stability concerning an acoustically excited drop in combustion products. *C. R. Mecanique Académie des* **sciences**. **342,** pp. 240–253, 2014. https://doi.org/10.1016/j.crme.2014.02.004

[xvii] Chandrasekhar, S.: Hydrodynamic and hydromagnetic stability, Clarendon, Oxford, 1961.

[xviii] Pearson, J.R.A.: On convection cells induced by surface tension, J. Fluid Mech., \textbf{4}, 489-500 (1958)

[xix] Scriven, L.E. Sternling, C.V.: On cellular convection driven by surface-tension gradients: effects of mean surface tension and surface viscosity, Chem. Engng. Mech., \textbf{19}, 321-340 (1964)

[xx] Abramzon, B. & Sirignano, W. A. (1989): Droplet vaporization model for spray combustion calculations, *Int. J. Heat Mass Transfer*, **32**, Nº 9, pp. 1605-1618. doi:10.1016/0017-9310(89)90043-4.

[xxi] Lamb, H.: *Hydrodynamics*, Cambridge University Press, Cambridge, 1945

[xxii] Johns, L.E., Beckmann, R.B. (1966): "Mechanism of dispersed-phase mass transfer in viscous, single-drop extraction system", *A.I.Ch.E. Jl* **12**(1), 10-16.

[xxiii] Mitsuaki Tanabea, Takuo Kuwahara, Kimiyoshi Satoh, Toshiro Fujimori, Junichi Sato, Michikata Kono. Droplet combustion in standing sound waves. Proceedings of the Combustion Institute **30** (2005) 1957–1964.

[xxiv] R. Prud'homme, M. Habiballah, L. Matuszewski, Y. Mauriot, and A. Nicole, *Theoretical analysis of dynamic response of a vaporizing droplet to an acoustic oscillation*, J. Propulsion and Power 26(1) (2010), pp. 74-83.

[xxv] K. Anani, R. Prud'homme, and M. N. Hounkonnou, *Dynamic response of a vaporizing spray to pressure oscillations: Approximate analytical solutions*, Combust. Flame 193 (2018), pp. 295-305.